Sub Topic: Laminar Flames

The 2018 (41st) Spring Technical Meeting
Organized by the Eastern States Section of the Combustion Institute (ESSCI)
and hosted by the Pennsylvania State University
State College, PA, March 4-7, 2018

Computational Simulations of Nonequidiffusive Premixed Flames in Obstructed Pipes

Abdulafeez Adebiyi[1], Gbolahan Idowu[1], Damir Valiev[2] and V'yacheslav Akkerman[1,*]

[1] *Computational Fluid Dynamics and Applied Multi-Physics Center*
Center for Innovation in Gas Research and Utilization (CIGRU)
Center for Alternative Fuels, Engines and Emissions (CAFEE)
Department of Mechanical and Aerospace Engineering, West Virginia University
Morgantown, WV 26506-6106, USA

[2] *Center for Combustion Energy, Tsinghua University, Beijing 100084, China*

[*] *Corresponding Author Email: Vyacheslav.Akkerman@mail.wvu.edu*

Abstract: The impact of the Lewis number, Le, on the dynamics and morphology of a premixed flame front, spreading through a toothbrush-like array of obstacles in a semi-open channel, is studied by means of the computational simulations of the reacting flow equations with fully-compressible hydrodynamics and Arrhenius chemical kinetics. The computational approach employs a cell-centered, finite-volume numerical scheme, which is of the 2nd-order accuracy in time, 4th-order in space for the convective terms, and of the 2nd-order in space for the diffusive terms. The channels of blockage ratios 0.33~0.67 are considered, with the Lewis numbers in the range $0.2 \le Le \le 2.0$ employed. It is shown that the Lewis number influences the flame evolution substantially. Specifically, flame acceleration weakens for $Le>1$ (inherent to fuel-lean hydrogen or fuel-rich hydrocarbon burning), presumably, due to a thickening of the flame front. In contrast, $Le<1$ flames (such as that of rich hydrogen or lean hydrocarbon) acquire an extra strong folding of the front and thereby accelerate even much faster. The later effect can be devoted to the onset of the diffusional-thermal combustion instability.

Keywords: **premixed combustion, nonequidiffusive flames, Lewis number, obstructed channels.**

1. Introduction

Flame acceleration (FA) and deflagration-to-detonation transition (DDT) are usually considered as the fire safety demands, but they are also expected to improve various advanced combustion technologies such as pulse- and rotation-detonation engines [1] or micro-combustors [2]. Among geometries associated with FA and DDT, obstructed pipes provide the fastest regime of burning [3]. While flame propagation through obstacles is oftentimes associated with turbulence, shocks [4], or hydraulic resistance [5], Bychkov *et al.* [6-9] identified a conceptually laminar, shockless mechanism of ultrafast FA in semi-open channels or tubes equipped with a toothbrush-like array of obstacles. This mechanism is illustrated in Fig. 1, and it is devoted to a powerful jet-flow along the channel centerline, generated by a cumulative effect of delayed combustion in the pockets between the obstacles. According to the analytical formulation [6], substantiated by the computational simulations [6,7,9], a flame accelerates in a two-dimensional (2D) channel as

$$\frac{U_{tip}}{S_L} = \Theta \exp\left[\frac{(\Theta-1)}{(1-\alpha)}\frac{S_L}{R}t\right] = \Theta \exp(\sigma\tau), \qquad \sigma = \frac{(\Theta-1)}{(1-\alpha)}, \tag{1}$$

where $U_{tip} \equiv dZ_{tip} / dt$ is the flame tip velocity in the laboratory reference frame, S_L the planar flame speed, $\Theta \equiv \rho_u / \rho_b$ the thermal expansion in the burning process, R the half-width of the channel, α the blockage ratio, and $\tau = S_L t / R$ the scaled time. This FA is extremely powerful indeed: say, for typical $\Theta = 8$ and $\alpha = 1/2$, the scaled exponential acceleration rate of Eq. (1) is $\sigma = (\Theta - 1)/(1-\alpha) = 14$! It is noted that σ drastically depends on α ; it grows with α and Θ, thereby promoting FA, but it does not depend on R. To some extent, this makes the Bychkov acceleration mechanism scale-invariant (Reynolds-independent) and, thereby, relevant to various scales, including micro-combustors, industrial conduits as well as mining and subway tunnels.

The theory and modelling [6] adopted a number of simplifications, including the conventional approach of equidiffusive combustion, when the Lewis number, defined as the thermal-to-mass diffusivities ratio is unity, $Le = 1$. However, $Le \neq 1$ oftentimes in the practical reality, which leads to the interplay between the internal and global flame structures such as the diffusional-thermal instability. The impact of Le on FA has been found substantial in *unobstructed* channels [10-12]. In particular, Bilgili *et al.* [12] has shown that FA in unobstructed channels is drastically promoted in a $Le < 1$ premixtures, due to enormous extra elongation ("channeling") of the flame front. In contrast, $Le > 1$ combustion leads to a flame "thickening", thereby moderating FA.

May we expect the same or similar impacts of Le in an obstructed channel? Answering this question constitutes the focus of the present work. Initially, we anticipated a similar effect for $Le > 1$ flames, but not in the case of $Le < 1$, because the obstacles were expected to prevent the flame channeling and, thereby, drastic elongation of the flame surface area, accompanied by FA. In contrast, we have found that the role of Le is significant in *both* cases, with moderation of acceleration for $Le > 1$ flames and strong promotion of FA in the case of $Le < 1$ combustion. In fact, the impact of the Lewis number is found to be as strong as that of the blockage ratio α .

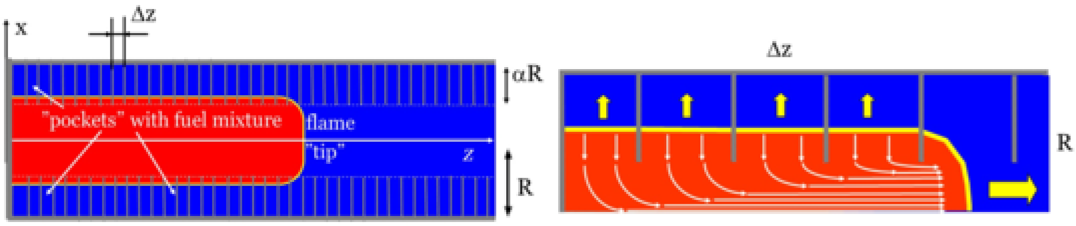

Figure 1: An illustration of the Bychkov mechanism of flame acceleration in an obstructed channel.

2. Numerical Method

We performed the computational simulations of the following 2D, Cartesian set of equations:

$$\frac{\partial}{\partial t}\rho + \frac{\partial}{\partial x_i}(\rho u_i) = 0, \qquad \frac{\partial}{\partial t}(\rho u_i) + \frac{\partial}{\partial x_j}\left(\rho u_i u_j + \delta_{i,j} P\right) - \gamma_{i,j} = 0, \tag{2}$$

$$\frac{\partial}{\partial t}\left(\rho \varepsilon + \frac{1}{2}\rho u_i u_j\right) + \frac{\partial}{\partial x_i}\left(\rho u_i h + \frac{1}{2}\rho u_i u_j u_j + q_i - u_j \gamma_{i,j}\right) = 0, \tag{3}$$

$$\frac{\partial}{\partial t}(\rho Y) + \frac{\partial}{\partial x_i}\left(\rho u_i Y - \frac{\zeta}{Sc}\frac{\partial Y}{\partial x_i}\right) = -\frac{\rho Y}{\tau_R}\exp\left(-E_a / R_p T\right), \tag{4}$$

where Y is the mass fraction of the fuel mixture; $\varepsilon = QY + C_V T$ and $h = QY + C_P T$ the specific internal energy and enthalpy, respectively; $Q = C_P T_f (\Theta - 1)$ the energy release in the reaction, with the specific heats at constant volume, C_V, and pressure, C_P, the initial fuel temperature,

$T_f = 300K$, pressure, $P_f = 1\text{bar}$, and density, $\rho_f = 1.16\,\text{kg/m}^3$. The stress tensor $\gamma_{i,j}$ and the energy diffusion vector q_i read

$$\gamma_{i,j} = \zeta\left(\frac{\partial u_i}{\partial x_j} + \frac{\partial u_j}{\partial x_i} - \frac{2}{3}\frac{\partial u_k}{\partial x_k}\delta_{i,j}\right), \qquad q_i = -\zeta\left(\frac{C_p}{\text{Pr}}\frac{\partial T}{\partial x_i} + \frac{Q}{\text{Sc}}\frac{\partial Y}{\partial x_i}\right), \tag{5}$$

where $\zeta \equiv \rho\nu$ is the dynamic viscosity, being $\zeta_f = 1.7\times10^{-5}\,kg/(\text{m}\cdot\text{s})$ in the fuel mixture. Then the thermal flame thickness can be defined, conventionally, as $L_f = \zeta_f / \text{Pr}\,\rho_f S_L = 4.22\times10^{-5}\,\text{m}$. As a result, Eqs. (2) – (5) include fully-compressible hydrodynamics, transport properties (heat conduction, diffusion and viscosity), and combustion imitated by a single irreversible Arrhenius reaction of the first order, with the activation energy E_a and the constant of time dimension τ_R. More details of the numerical scheme and the solver can be found, for instance, in Refs. [6,7,9].

Similar to Fig. 1, the flame propagates in a long 2D channel of width $2R$, where the fraction $2R\alpha$ is blocked by the obstacles with spacing (the distance between two neighboring obstacles) Δz. The channel width is described by the Reynolds number associated with flame propagation, $\text{Re} \equiv RS_L/\nu = R/\text{Pr}\,L_f = R/L_f$. In the present work, we used $\Delta z/R = 1/4$, $\text{Re} = 24, 36, 48$, and $\alpha = 1/3; 1/2; 2/3$. The walls of the channel and obstacles are adiabatic, $\mathbf{n}\cdot\nabla T = 0$, and free-slip, $\mathbf{n}\cdot\mathbf{u} = 0$, where $\mathbf{n}$ is the normal vector at the wall. The absorbing (non-reflecting) boundary conditions are employed at the open end to prevent the reflection of the sound waves and weak shocks. The left end of the free part of the channel is closed while the other end, on the right, is open, with the boundary conditions $\rho = \rho_f$, $P = P_f$, $u_z = 0$ adopted. The initial flame structure is imitated by the classical Zeldovich-Frank-Kamenetsky (ZFK) solution for a hemispherical flame front [7], of initial radius $5.1L_f$, ignited at the centerline, and the closed end of the channel.

Both the fuel mixture and burnt matter are assumed to be ideal gases of constant molecular weight, $M = 29$ kg/kmol, such that the equation of state is $P = \rho R_P T/M$, with the universal gas constant $R_P = 8.31\,\text{kJ}/(\text{kmol}\cdot\text{K})$. The chemical properties of the fuel mixture are chosen to model methane-air burning with a Lewis number in the range $0.2 \le Le \le 2.0$, thermal expansion $\Theta = 8$, and the planar flame speed $S_L = 34.7$ cm/s. The initial speed of sound in this fuel mixture is 10^3 times larger, $c_0 = 347$ m/s, such that hydrodynamics is almost incompressible at the initial stage of burning. In this respect, in addition to the standard scaling of Eq. (1), U_{tip}/S_L, we also scaled U_{tip} by the local, instantaneous speed of sound, $c_{tip} = \sqrt{(c_p/c_v)\times(R_p/M)\times T_{tip}}$. Such a flame tip Mach number $M_{tip}(t) \equiv U_{tip}/c_{tip}$ appears a good measure of the current level of compressibility as well as of the instantaneous stage of the DDT process, being $M_{tip} << 1$ at the initial, quasi-isobaric stage of burning and approaching an order of unity by the time of detonation triggering.

3. Results and Discussion

We have performed extensive computational simulations of premixed FA in the configuration described above, and for various Le, α and Re. Because of the limit of space, we present only a single combination of color temperature snapshots, but, presumably, the most illustrative. Figure 2 (a-i) shows the flame shapes and positions attained at various Le, $Le = 0.2, 1.0, 2.0$, and α, $\alpha = 1/3; 1/2; 2/3$ but at the *same time instant*, $\tau = 0.075$, and for the same $\text{Re} = 24$ in all nine simulation runs. The respective $M_{tip}|_{\tau=0.075}$ are also depicted. The flames are represented by the color temperature snapshots, from 300 K in the fuel (blue) till 2400 K in the burnt matter (red). It is seen that the role of the Lewis number is paramount and as strong as that of the blockage ratio. Indeed, when both the effect of large α and nonequidiffusivity (with $Le < 1$) work together, as in Fig. 2c for $\alpha = 2/3$ and $Le = 0.2$, then the flame front is drastically fold; it has propagated through $17R$ and is, presumably, about to trigger detonation as the flame tip Mach number is as high as $M_{tip} = 0.6$. Consequently, FA is enormous in this case. In contrast, a $Le > 1$ flame in a channel with small blockage ratio accelerates very slow, as observed in Fig. 2g for $\alpha = 1/3$ and $Le = 2.0$. In other cases of Fig. 2, the effects of α and Le compete such that we observe almost equivalent flames and M_{tip} in the pairs 2d and 2h; 2a and 2e; an even 2b and 2i, respectively.

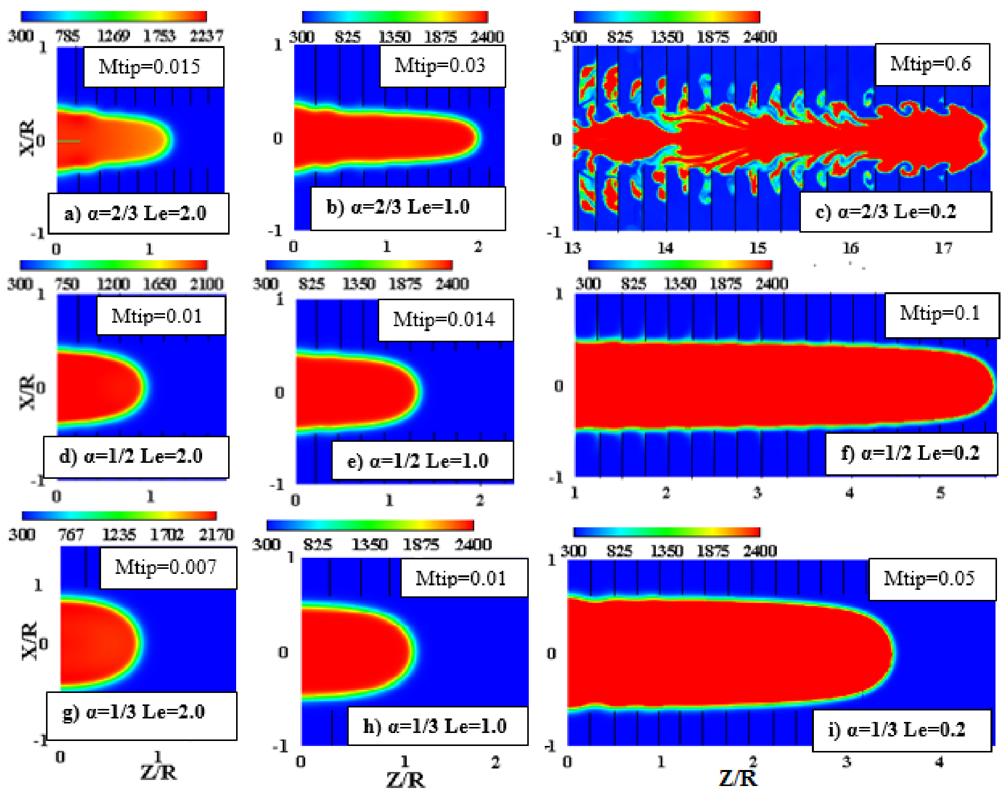

Figure 2: Color temperature snapshots [from 300 K in the fuel (blue) till 2400 K in the burnt matter (red)] taken at the same scaled time $\tau = tS_L/R = 0.075$ for Re = 24 and various Le = 0.2, 1.0, 2.0 and α = 1/3; 1/2; 2/3.

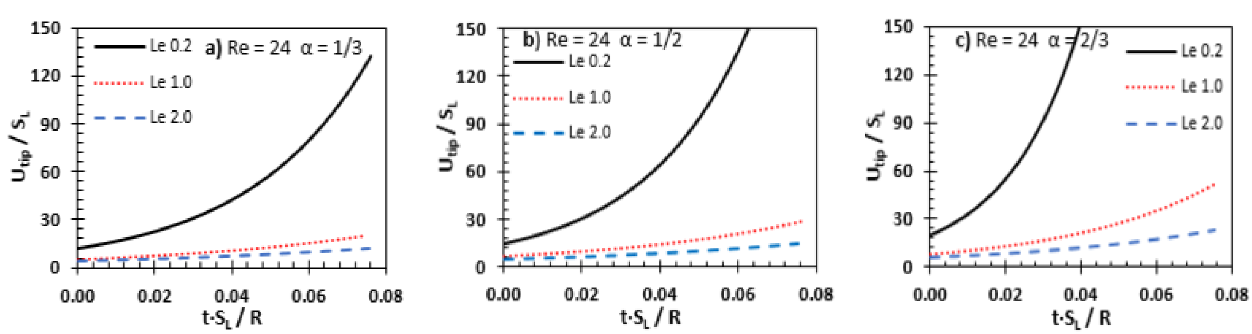

Figure 3: The scaled flame tip U_{tip}/S_L vs the scaled time τ for Re = 24 and α = 1/3 (a), 1/2 (b), and 2/3 (c).

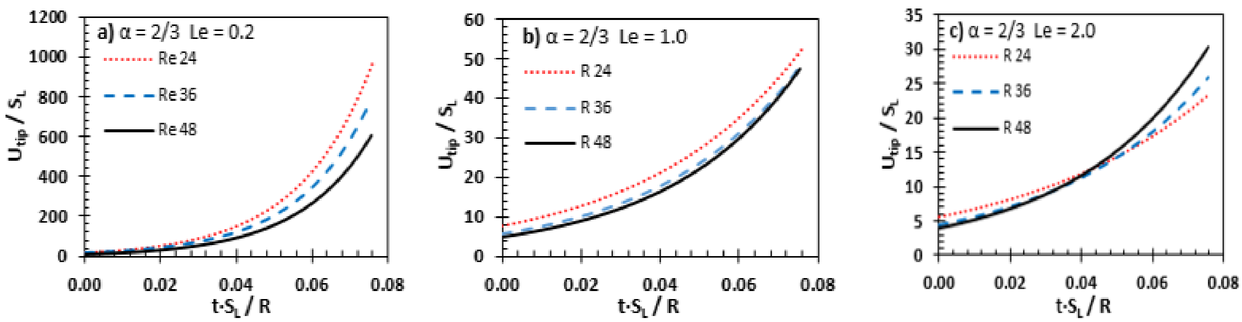

Figure 4: The scaled flame tip velocity U_{tip}/S_L vs the scaled time τ for α = 2/3 and *Le* = 0.2 (a), 1.0 (b), and 2.0 (c).

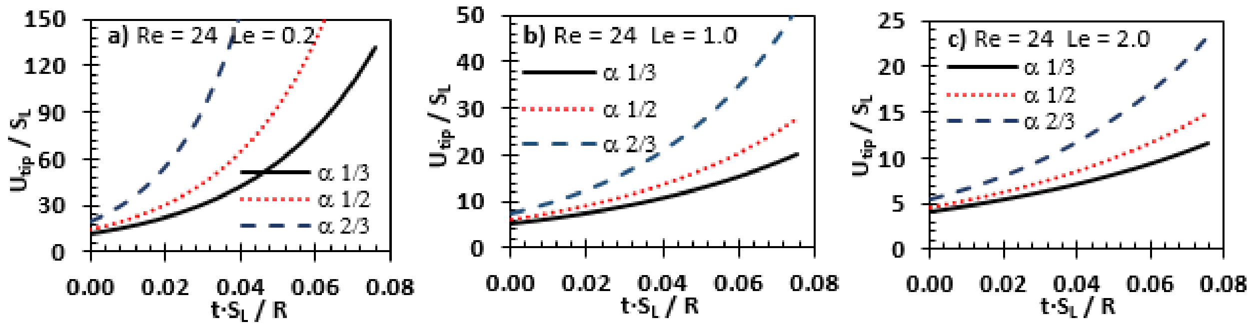

Figure 5: The scaled flame tip velocity U_{tip}/S_L vs the scaled time τ for Re = 24 and *Le* = 0.2 (a), 1.0 (b), and 2.0 (c).

To quantify the impact of *Le*, in Fig. 3 we present the time evolution of the scaled flame tip velocity, U_{tip}/S_L, for several blockage ratios, α = 1/3 (3a), 1/2 (3b), and 2/3 (3c), with various *Le*, *Le* = 0.2, 1.0, 2.0 in each plot. It is seen that the effect of *Le* is very strong, especially for the *Le* < 1 flames. Indeed, in all three Figs. 3(a-c), *Le* = 0.2 promotes U_{tip} almost by an order of magnitude as compared to the equidiffusive case, *Le* = 1. The effect of Le > 1 is substantially weaker, but *Le* = 2.0, nevertheless, noticeably moderates FA as compared to the *Le* = 1 cases.

Figure 4 scrutinizes the role of the channel width for various *Le* and α. It is seen that the impact of Re is minor as all the curves for Re = 24, 36 and 48 go very close in all three Figs. 4 (a-c). This actually supports the Bychkov formulation [6] predicting Re-independent FA, Eq. (1). On the other hand, Fig. 4 shows a very intriguing result: even the Re-dependence is quite weak, the impact of *Le* may change it, up to the opposite one. Indeed, FA weakens with Re for *Le* ≤ 1 flames, Fig. 4(a, b), but it is promoted with Re in the *Le* > 1 case, Fig. 4c. In this light, we can potentially look for a certain threshold *Le* that would correspond to the change of the trend and thus provide the complete Re-independence.

Figure 5 shows the role of the blockage ratio α. It is seen that α-dependence is significant and much stronger than Re-dependence for all *Le* considered. At the same time, the impact of *Le* on α-dependence is less than that on Re-dependence: α-dependence does not change sign due to *Le*, but there is a noticeably quantitative effect such that α-dependence is stronger for *Le* < 1 flames.

Finally, we have studied all the acceleration trends observed, and when acceleration exhibited an exponential trend, then the exponential acceleration rate was calculated. The result is plotted versus *Le* in Fig. 6, for Re = 24, 36 and 48 in Figs. 6 (a-c), respectively, with α = 1/3, 1/2 and 2/3 in each figure. As expected, the acceleration rate σ appears largest for non-equidiffusive cases of *Le* < 1. More specifically, the exponential acceleration trend is seen for *Le* = 0.2 only for low α, α = 1/3, 1/2. The absence of this trend for α = 1/2 is attributed to a strong competition between the *Le* and α effects in that scenario.

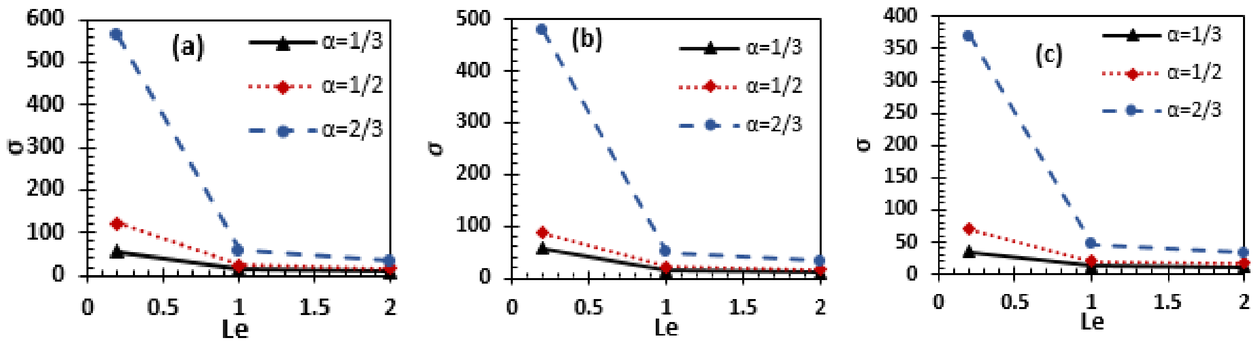

Figure 6: The exponential acceleration rate σ vs the Lewis number *Le* for Re = 24 (a), 36 (b), and 48 (c), with α = 1/3, 1/2, and 2/3 in each figrure.

4. Conclusions

In this work, a thorough investigation of non-equidiffusive FA in obstructed channels has been performed, by means of computational simulations, and a profound impact of *Le* on FA has been identified. This effect is compared to that of α and it has been found to be as strong. The non-equidiffusive scenarios involve non-unity *Le*, such that in the case of *Le* < 1, promotion of flame acceleration is discovered. It is found that *Le* influences α-dependence. In contrast, moderation of FA has been observed for *Le* > 1 flames. In addition, a unique trend is noticed for the *Le*-impact on Re. Indeed, the Lewis number may change Re-dependence of FA to an opposite trend.

Finally, we aim to unify the analysis. Similar to Bychkov *et al.* [6], the combination $\sigma Z_f / \Theta R$ is plotted versus $\sigma t S_L / R$ in Fig. 7. Here, different colors represent different Lewis numbers (blue, orange and grey for *Le* = 0.2, 1.0 and 2.0, respectively), with three blockage ratios for each case, namely α = 1/3 (solid), 1/2 (dashed) and 1/3 (dotted). While Ref. [6] was limited to equidiffusive flames, *Le* = 1, with all the data collapsing into a single curve; here we have various *Le*, and the set of curves associated with different *Le* (i.e. different colors) differ. However, for each given *Le*, the plots (of the same color) collapse into a single curve, thereby fitting the Bychkov model.

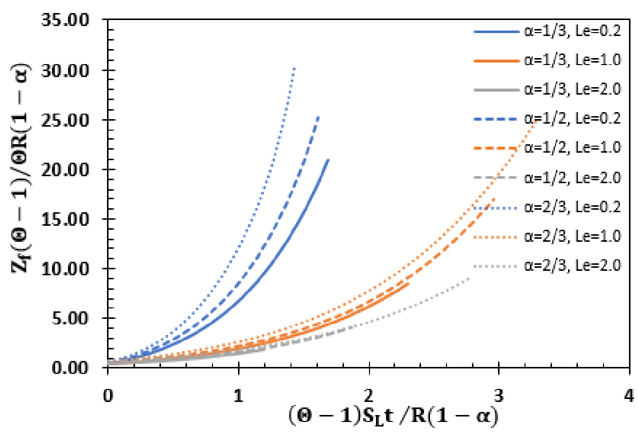

Figure 7: Scaled flame tip position $\sigma Z_f / \Theta R$ vs the scaled time $\sigma t S_L / R$ for various *Le* = 0.2 (blue), 1.0 (orange) and 2.0 (grey), with three different α = 1/3 (solid), ½ (dashed) and 2/3 (dotted) for each given *Le*.

5. Acknowledgements

This research was funded by the NSF through the CAREER Award No. 1554254 (V.A.).

6. References

[1] G. Roy, S. Frolov, A. Borisov, D. Netzer, Prog. Energy Combust. Sci. 30 (2004) 545.
[2] Y. Ju, K. Maruta, Prog. Energy Combust. Sci. 37 (2011) 669.
[3] E.S. Oran, V.N. Gamezo, Combust. Flame 148 (2007) 4.
[4] G. Ciccarelli, S. Dorofeev, Prog. Energy Combust. Sci. 34 (2008) 499.
[5] I. Brailovsky, L. Kagan, G. Sivashinsky, Phil. Trans. R. Soc. A 370 (2012) 625.
[6] V. Bychkov, D. Valiev, L.-E. Eriksson, Phys. Rev. Lett. 101 (2008) 164501.
[7] D. Valiev, V. Bychkov, V. Akkerman, C.K. Law, L.-E. Eriksson, Combust. Flame 157 (2010) 1012.
[8] V. Bychkov, V. Akkerman, D. Valiev, C.K. Law, Combust. Flame 157 (2010) 2008.
[9] O. Ugarte, V. Bychkov, J. Sadek, D. Valiev, V. Akkerman, Phys. Fluids 28 (2016) 093602.
[10] J.B. Bell, R.K. Cheng, M.S. Day, I.G. Shepherd, Proc. Combust. Inst. 31 (2007) 1309.
[11] C. Cui, M. Matalon, T.L. Jackson, AIAA Journal 43 (2005) 1284.
[12] S. Bilgili, D. Valiev, V. Bychkov, V. Akkerman, 9th U.S. National Combustion Meeting, May 17-20, 2015, paper #3E08, pp. 1-10.